NON-UNIFORM PHASES IN A THREE-FLAVOUR 't HOOFT EXTENDED NAMBU–JONA-LASINIO MODEL*

J. Moreira, B. Hiller

Centro de Física Computacional, Department of Physics
University of Coimbra, 3004-516 Coimbra, Portugal

W. Broniowski

The Henryk Niewodniczański Institute of Nuclear Physics
Polish Academy of Sciences, 31-342 Kraków, Poland
and
Institute of Physics, Jan Kochanowski University, 25-406 Kielce, Poland

A.A. Osipov, A.H. Blin

Centro de Física Computacional, Department of Physics
University of Coimbra, 3004-516 Coimbra, Portugal

(Received December 5, 2014)

The possible existence of non-uniform phases in cold dense quark matter in the light quark sector (u, d, s) is addressed within the Nambu–Jona-Lasinio Model extended to include the flavour-mixing 't Hooft determinant. The effect of changes in the coupling strengths of the model is discussed. It is seen that the inclusion of the strange sector catalyses the appearance of the non-uniform phases, extending the domain for their existence.

DOI:10.5506/APhysPolBSupp.8.191
PACS numbers: 11.30.Rd, 11.30.Qc, 12.39.Fe, 21.65.Qr

1. Introduction

It has been proposed long ago (for recent reviews, see [1]) that the non-trivial dynamics due to the attractive interaction of pions with quarks (or nucleons) allows for the existence of non-uniform phases in the low temperature and high chemical potential regime of the QCD phase diagram. As the

* Talk presented by J. Moreira at the EEF70 Workshop on Unquenched Hadron Spectroscopy: Non-Perturbative Models and Methods of QCD *vs.* Experiment, Coimbra, Portugal, September 1–5, 2014.

sign problem affects lattice QCD at non-zero baryon density, the use of alternative approaches such as low energy models of the Nambu–Jona-Lasinio (NJL) [3] type, became a useful exploratory tool in the studies of strongly interacting matter.

In this paper, we outline some results reported in detail in [4], pertaining to the study of the NJL model with the 't Hooft determinant [5] applied to the case, where the light quark chiral condensates assume the shape of the chiral wave. We work at zero temperature and in the chiral limit for the u and d sector, while the s quark has a non-vanishing current mass.

2. The model

The chiral wave *ansatz* proposed in [6], with the corresponding quark orbitals and energy levels, forms a self consistent solution of the Euler–Lagrange equations of the model in the chiral limit. They have the form

$$\begin{aligned} \langle \overline{\psi_l}\psi_l \rangle &= \frac{h_l}{2}\cos(\boldsymbol{q}\cdot\boldsymbol{r})\,, \qquad \langle \overline{\psi_l} i\gamma_5\tau_3\psi_l \rangle = \frac{h_l}{2}\sin(\boldsymbol{q}\cdot\boldsymbol{r})\,, \\ E^{\pm} &= \sqrt{M^2+p^2+\frac{q^2}{4} \pm \sqrt{(\boldsymbol{p}\cdot\boldsymbol{q})^2+M^2q^2}}\,, \end{aligned} \tag{1}$$

where τ_3 is the Pauli matrix acting in the isospin space, M is the quark dynamical mass, $\boldsymbol{p}$ denotes the momentum of the quark, and $\boldsymbol{q}$ is the wave vector of the condensate modulation. We choose the z-axis to coincide with $\boldsymbol{q}$ (note that the E^- branch has a lower energy than E^+). For the s quark, a uniform condensate background is considered.

The application of techniques of Ref. [7] yields the thermodynamic potential of the model in the mean field approximation as

$$\begin{aligned} \Omega &= V_{\rm st} + \frac{N_c}{8\pi^2}\left(J_{-1}(M_u,\mu_u,q)+J_{-1}(M_d,\mu_d,q)+J_{-1}(M_s,\mu_s,0)\right)\,, \\ V_{\rm st} &= \frac{1}{16}\left(4G\left(h_u^2+h_d^2+h_s^2\right)+\kappa h_u h_d h_s\right)\Big|_0^{M_i}\,, \end{aligned} \tag{2}$$

where h_i $(i=u,d,s)$ are twice the quark condensates. The integrals J_{-1} stem from the fermionic path integral over the quark bilinears which appear after bosonization, while $V_{\rm st}$ corresponds to the stationary phase contribution to the integration over the auxiliary bosonic fields. The NJL coupling strength is G, while κ is the OZI-violating 't Hooft determinant coupling. From the value evaluated at the dynamical masses M, a subtraction of its value evaluated at $M=0$ is made [8] (denoted by the $|_0^M$ symbol in Eq. (2)). We use a regularized kernel corresponding to two Pauli–Villars subtractions in the integrand [9], namely $\rho\left(s\Lambda^2\right)=1-(1+s\Lambda^2)\exp(-s\Lambda^2)$. The Dirac

and Fermi sea contributions, $J_{-1}^{\rm vac}$ and $J_{-1}^{\rm med}$, can be written explicitly as

$$
\begin{aligned}
J_{-1} &= J_{-1}^{\rm vac} + J_{-1}^{\rm med}\,, \\
J_{-1}^{\rm vac} &= \int \frac{d^4p_{\rm E}}{(2\pi)^4} \int_0^\infty \frac{ds}{s} \rho\left(s\Lambda^2\right) 8\pi^2 e^{-s\left(p_{0\,\rm E}^2 + p_\perp^2\right)} \\
&\quad \times \left(e^{-s\left(\frac{q}{2} + \sqrt{M^2+p_z^2}\right)^2} + e^{-s\left(\frac{q}{2} - \sqrt{M^2+p_z^2}\right)^2} \right) \Big|_{0,0}^{M,q}\,, \\
J_{-1}^{\rm med} &= -\int \frac{d^3p}{(2\pi)^3} 8\pi^2 T \left(\mathcal{Z}_+^+ + \mathcal{Z}_-^+ + \mathcal{Z}_+^- + \mathcal{Z}_-^-\right)\Big|_{0,0}^{M,q} + C(T,\mu)\,, \\
\mathcal{Z}_\pm^\pm &= \log\left(1 + e^{-\frac{E^\pm \mp \mu}{T}}\right) - \log\left(1 + e^{-\frac{E_\Lambda^\pm \mp \mu}{T}}\right) - \frac{\Lambda^2}{2TE_\Lambda^\pm} \frac{e^{-\frac{E_\Lambda^\pm \mp \mu}{T}}}{1 + e^{-\frac{E_\Lambda^\pm \mp \mu}{T}}}\,, \\
C(T,\mu) &= \int \frac{d^3p}{(2\pi)^3} 16\pi^2 T \log\left(\left(1 + e^{-\frac{|\boldsymbol{p}|-\mu}{T}}\right)\left(1 + e^{-\frac{|\boldsymbol{p}|+\mu}{T}}\right)\right)\,, \qquad (3)
\end{aligned}
$$

where $E_\Lambda^\pm = \sqrt{(E^\pm)^2 + \Lambda^2}$. The $|_{0,0}^{M,q}$ notation refers to the subtraction of the same quantity evaluated for $M = 0$ and $q = 0$, which is done to set the zero of the potential at a uniform gas of massless quarks. The superscript $\pm$ in the definition of $\mathcal{Z}$ refers to the energy branch, whereas the subscript refers to the sign in front of the chemical potential in the exponent. The $C(T,\mu)$ term is needed for thermodynamic consistency [8]. The minimization of the Ω with respect to M and q has to be done self-consistently with the resolution of the following stationary phase equations (where m_i stands for the current masses of the quarks):

$$
\begin{cases}
m_u - M_u = G h_u + \frac{\kappa}{16} h_d h_s \\
m_d - M_d = G h_d + \frac{\kappa}{16} h_u h_s \\
m_s - M_s = G h_s + \frac{\kappa}{16} h_u h_d
\end{cases}\,. \qquad (4)
$$

3. Results

In our study, we chose the parameters to reproduce a reasonable value for the vacuum dynamical mass of the light quarks ($M_l = 300$ MeV). The current masses were set to $m_u = m_d = 0$, $m_s = 186$ MeV, the remaining three parameters of the model (G, κ and Λ) can be then reduced to two: the 't Hooft coupling strength, κ, and the dimensionless curvature, $\tau = N_c G \Lambda^2/(2\pi^2)$. In the chiral limit, $\tau = 1$ is the critical value above which dynamical chiral symmetry breaking occurs as a crossover for $1 < \tau < 1.23$ and as a first order transition for higher values.

With no OZI-violating term, the light and strange sectors are decoupled: two independent first order transitions occur for the light and strange sector, with the latter shifted to higher μ due to the current s-quark mass (both occur at values of μ close to the vacuum dynamical mass $M_i^{\rm vac}$). At high enough μ, the energetically favourable solution is always a modulated one, with a non-vanishing q — the non-uniform phase develops. Asymptotically, this solution goes to $\lim_{\mu\to\infty}\{h,q\} = \{0, 2\mu\}$ and becomes degenerate with the trivial one. Above $1.23 < \tau < 1.53$, a window for energetically favourable finite-q solutions appears in the vicinity of the first order transition encompassing it; the transition is not to a vanishing condensate, but $\{h_l, 0\} \to \{h_l', q\}$. The window ends with the light condensate going continuously to zero. For $\tau > 1.53$, this windows extends and merges with the one at higher chemical potentials.

Turning on flavour mixing couples the u–d and strange sectors. At fixed curvature, we find several different scenarios depending on the value of κ, as seen in Fig. 1 where we show the $\tau = 1.4$ case. For $-\kappa > 290$ GeV^{-5}, a new solution branch appears, with a shark-fin shape for h_l in the vicinity of $\mu \sim M_s^{\rm vac}$ (see the first row of Fig. 1). There are, therefore, three intervals

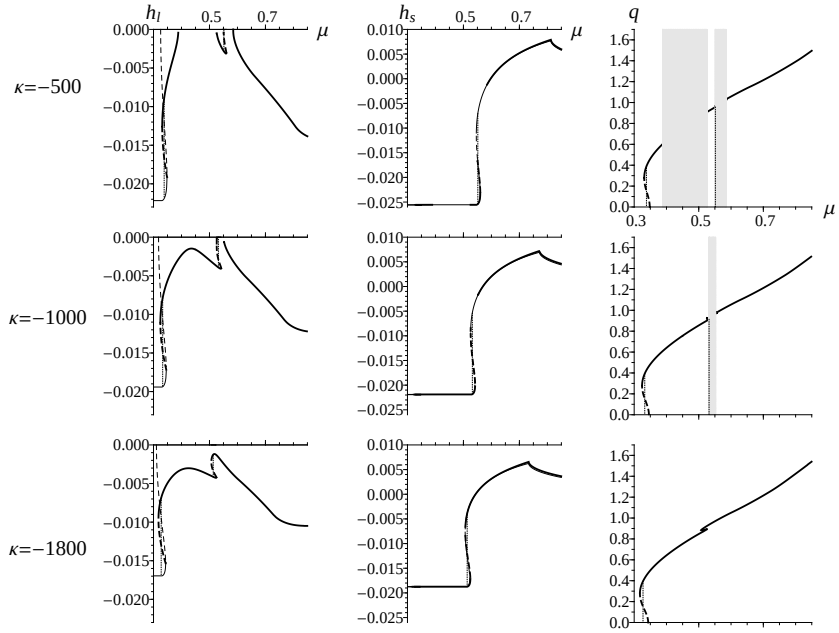

Fig. 1. The μ-dependence of h_l, h_s and q. Each row corresponds to a different value of the 't Hooft coupling strength ($[\kappa] = \text{GeV}^5$). Thicker lines denote the finite-q solutions. In the grey regions, the value of q is undetermined, since $h_l = 0$.

of μ where an energetically favourable finite-q solution exists. They are delimited by two first-order transitions and three crossovers (the crossovers correspond to the disappearance/emergence of a non-vanishing h_l). The two first-order transitions occur slightly below (for the one taking place near $M_l^{\rm vac}$) and slightly above (near $M_s^{\rm vac}$), thus excluding the occurrence of the $q = 0$ transitions. A zoom of the behaviour of the chiral condensates near the transitions can be seen in Fig. 2. For $-\kappa > 935$ GeV^{-5}, the first two μ windows with finite-q solutions merge, resulting in the disappearance of the corresponding crossover transitions, as can be seen in the second row of Fig. 1. With $-\kappa > 1660$ GeV^{-5}, the last transition to a vanishing q solution does not occur and is substituted by a first-order transition between the two phases with finite q (third row of Fig. 1 and Fig. 3). The dependence on κ of these critical chemical potentials can be seen in Fig. 4.

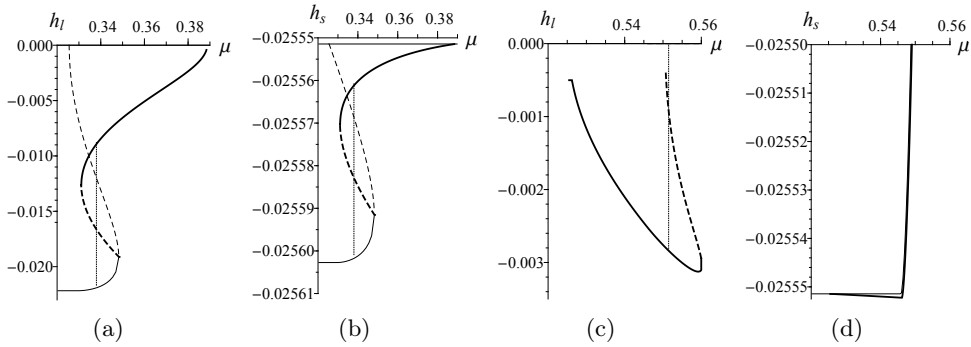

Fig. 2. Zoom for the chemical potential dependence of the chiral condensate solutions (thicker lines refer to finite-q solutions) near the transitions (marked by the vertical dotted lines), case of $\kappa = -500$ GeV^{-5}.

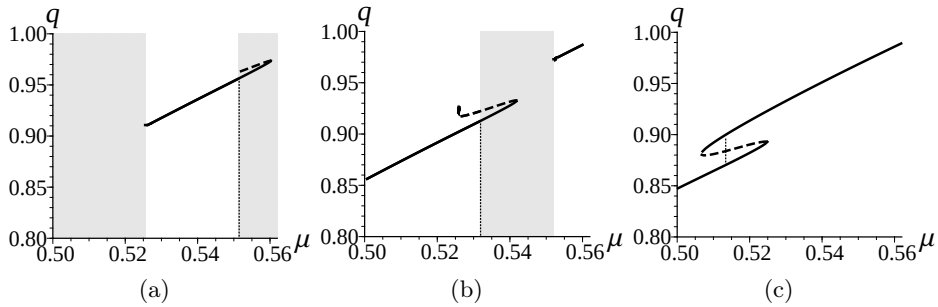

Fig. 3. Zoom of the solutions for q in the chemical potential window close to $M_s^{\rm vac}$ for $\kappa = -500, -1000$, and -1800 GeV^5 (from left to right).

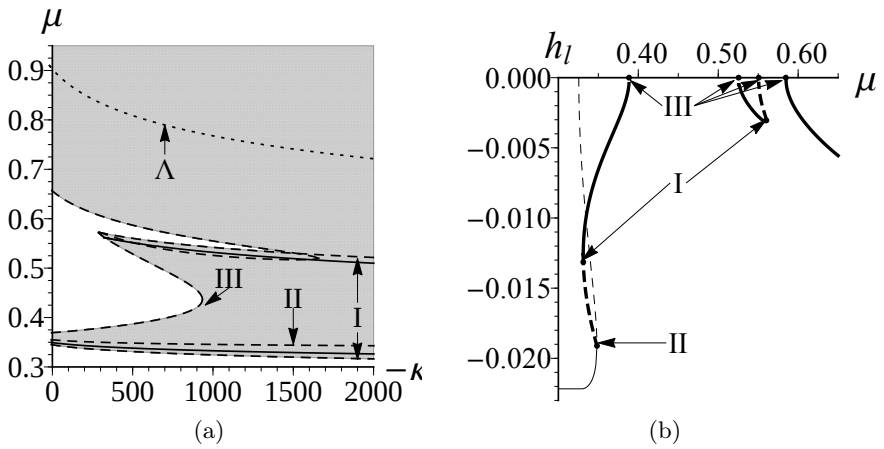

Fig. 4. Critical chemical potentials (in GeV) as functions of κ ($[\kappa] = \mathrm{GeV}^5$). The upper dotted line corresponds to the cut-off Λ. The chemical potential of the first order transitions are marked with the solid black lines. Dashed lines indicate the borders of the region where the finite-q solutions exist. We distinguish between three types of critical chemical potentials and an example for this distinction in the $\kappa = -500\ \mathrm{GeV}^{-5}$ case appears in Fig. 4(b) (type I with finite q and h_l, type II with finite h_l and vanishing q, and type III with finite q but vanishing h_l).

We conclude that the flavour mixing acts as a catalyst for the emergence of globally stable inhomogeneous solutions in zero-temperature quark matter.

This work has been supported by the Centro de Física Computacional of the University of Coimbra, the Fundação para a Ciência e Tecnologia, project: CERN/FP/116334/2010 and the grant SFRH/BPD/63070/2009/. This research is part of the EU Research Infrastructure Integrating Activity Study of Strongly Interacting Matter (HadronPhysics3) under the 7th Framework Programme of EU, Grant Agreement No. 283286. W.B. acknowledges the support of the Polish National Science Centre, grants DEC-2011/01/B/ST2/03915 and DEC-2012/06/A/ST2/00390.

REFERENCES

[1] W. Broniowski, *Acta Phys. Pol. B Proc. Suppl.* **5**, 631 (2012).

[2] M. Buballa, S. Carignano, `arXiv:1406.1367 [hep-ph]`.

[3] Y. Nambu, *Phys. Rev. Lett.* **4**, 380 (1960); *Phys. Rev.* **122**, 345 (1961); **124**, 246 (1961); V.G. Vaks, A.I. Larkin, *Sov. Phys. JETP* **13**, 192 (1961).

[4] J. Moreira *et al.*, *Phys. Rev.* **D89**, 036009 (2014).

[5] G. 't Hooft, *Phys. Rev.* **D14**, 3432 (1976).
[6] F. Dautry, E. Nyman, *Nucl. Phys.* **A319**, 323 (1979).
[7] A.A. Osipov, B. Hiller, *Eur. Phys. J.* **C35**, 223 (2004).
[8] B. Hiller *et al.*, *Phys. Rev.* **D81**, 116005 (2010).
[9] A.A. Osipov, M.K. Volkov, *Sov. J. Nucl. Phys.* **41**, 500 (1985).